Modeling TXS 0506+056 for AMEGO-X

Tiffany R. Lewis

NPP Fellow at NASA Goddard's Astroparticle Physics Lab

Collaborators: Christopher Karwin, Tonia Venters, Henrike Fleischhack, Yong Sheng, Carolyn Kierans, Regina Caputo, Julie McEnery

10th International Fermi Symposium

10 October 2022

tiffanylewisphd@gmail.com

Models for Blazar Jets

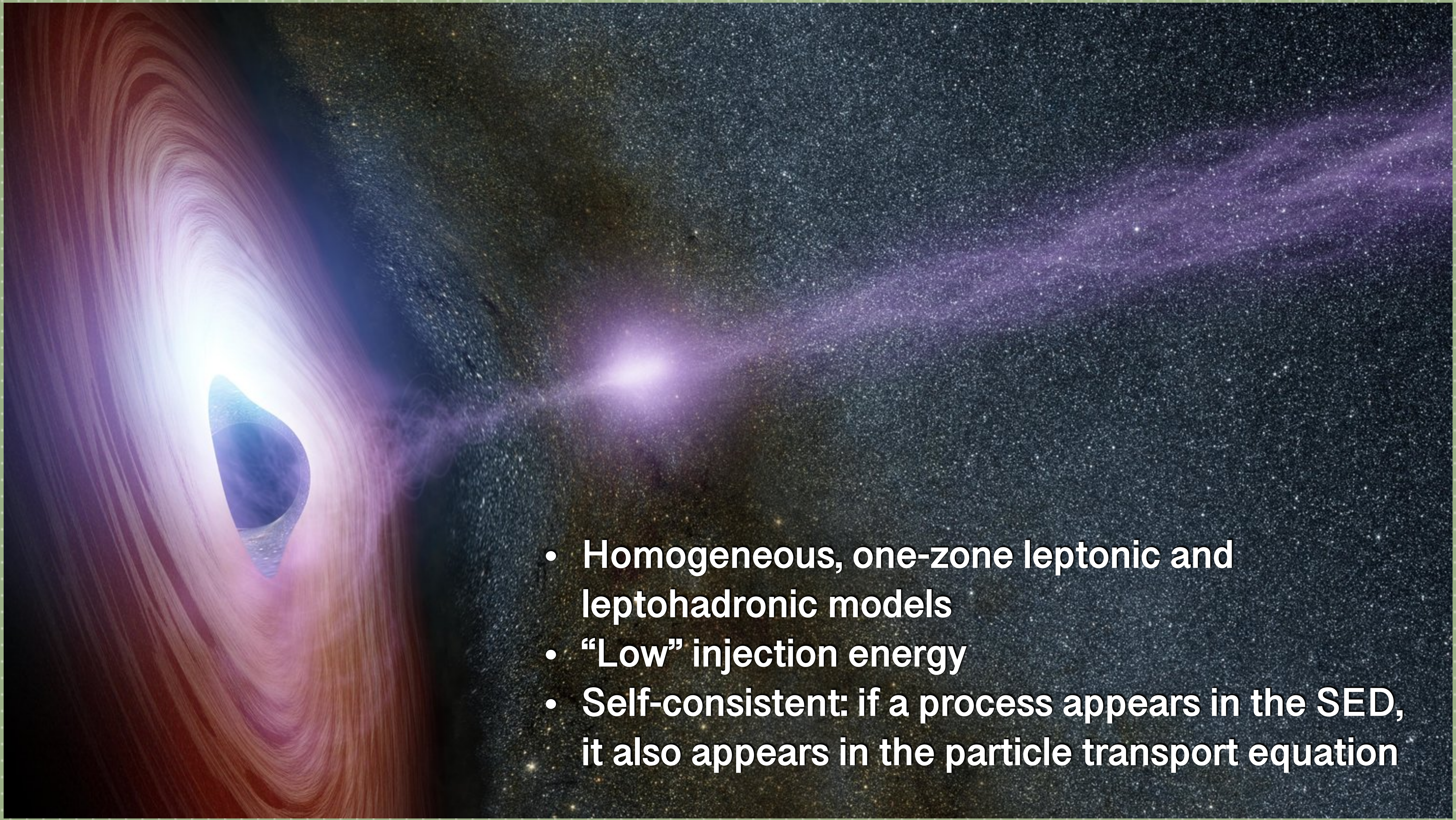

- Homogeneous, one-zone leptonic and leptohadronic models
- “Low” injection energy
- Self-consistent: if a process appears in the SED, it also appears in the particle transport equation

Image Credit: IPAC CalTech

Particle Acceleration Mechanisms: 1st & 2nd Order Fermi Interactions

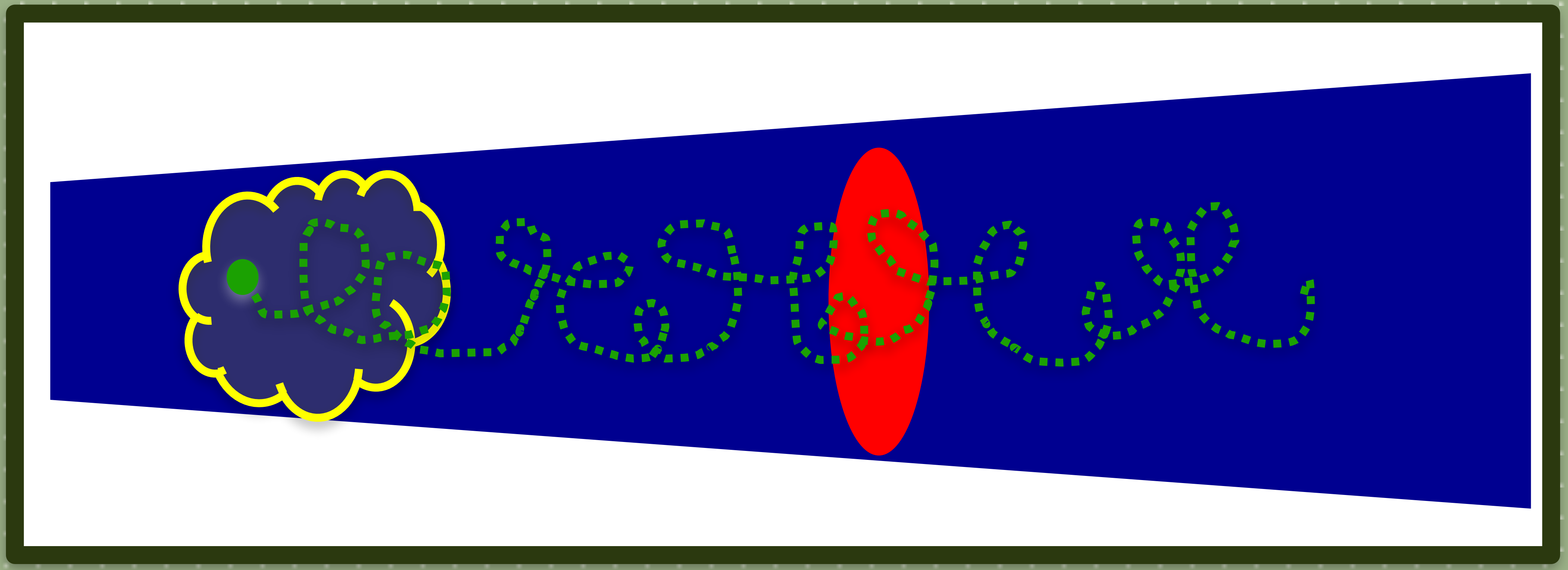

Fermi I:

Shock Acceleration (+) & Adiabatic Expansion (-)

Particles gain energy from shock crossings in proportion to the energy they already have, and can pass through a shock region multiple times

Fermi II:

Hard-Sphere Scattering off of Stochastic MHD Waves

Particles always gain energy from stochastic scatterings in the head-on approximation due to the bulk motions in the jet.

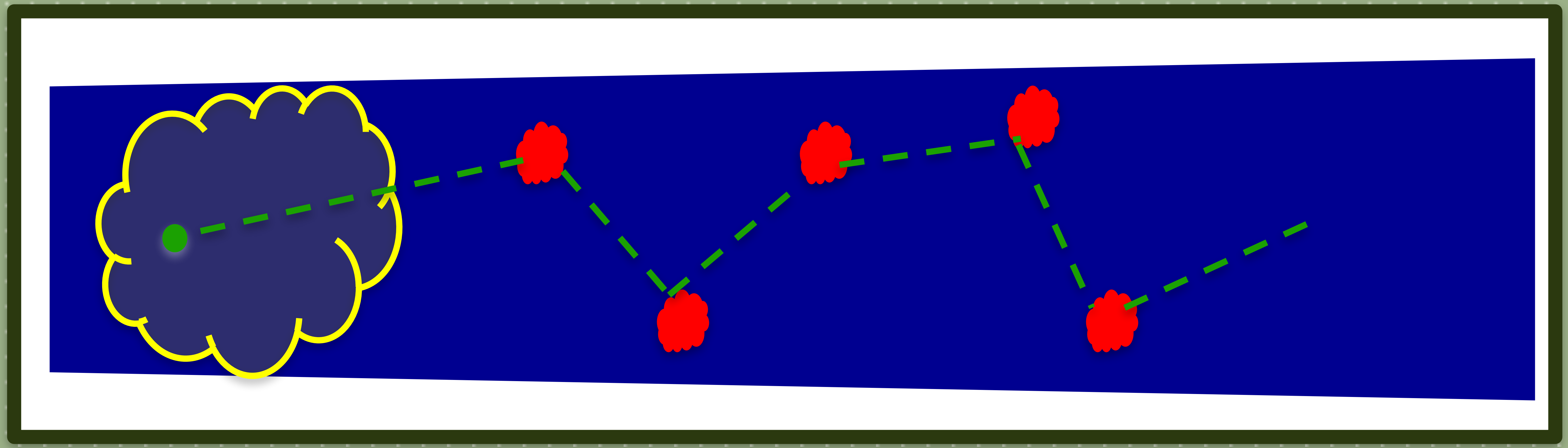

Particle Energy Loss Mechanisms: Synchrotron, Inverse Compton, Photo-pion Cascade

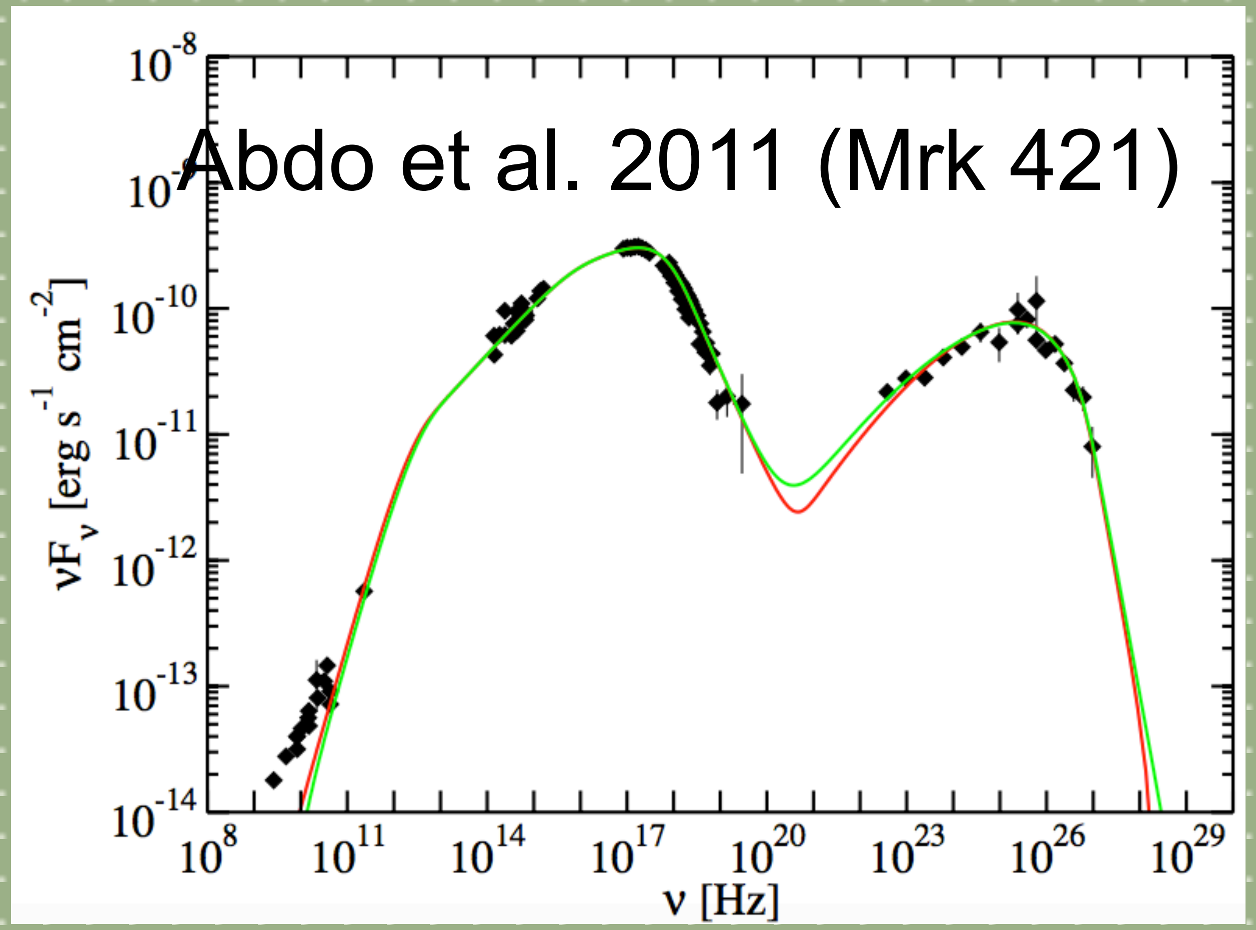

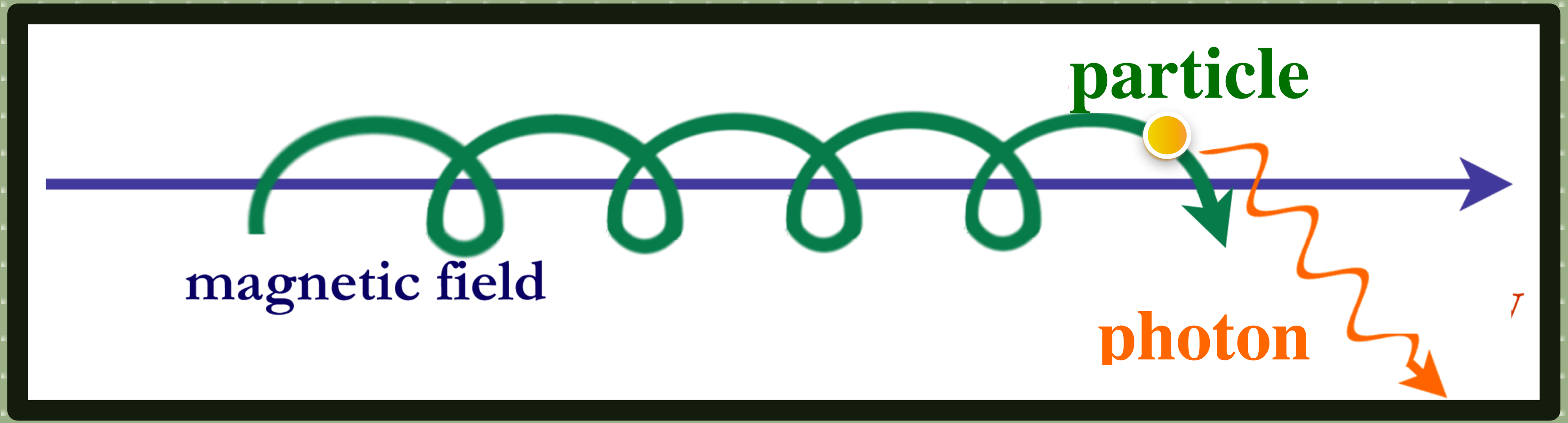

- Both electrons and protons populations can cool through synchrotron radiation.
- The rate of synchrotron cooling depends on the strength of the magnetic field.

Illustration: CXC/S. Lee

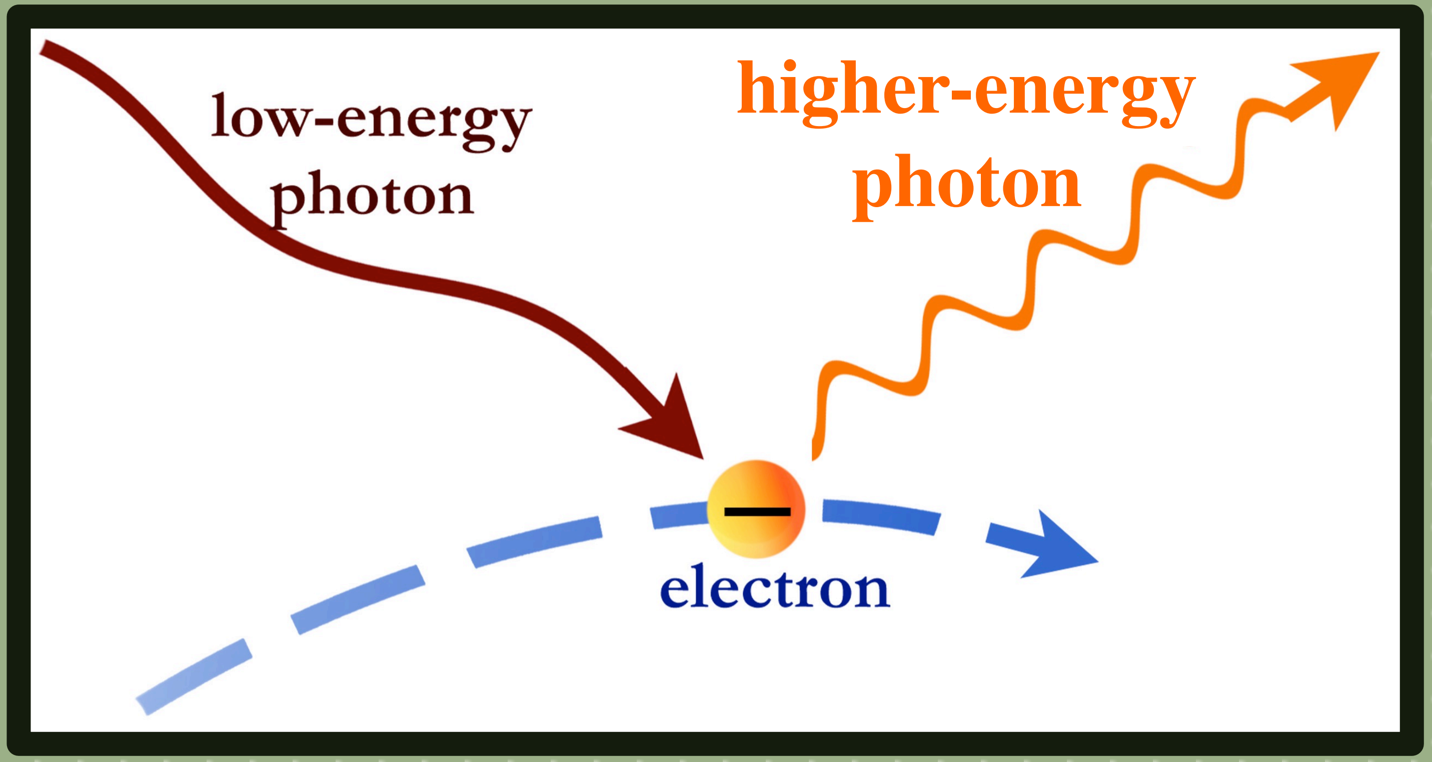

- Compton cooling describes the high-frequency SED bump in the leptonic picture.
- The Compton cooling rate depends on the energy density of the 'low-energy' photon field

Illustration: CXC/S. Lee

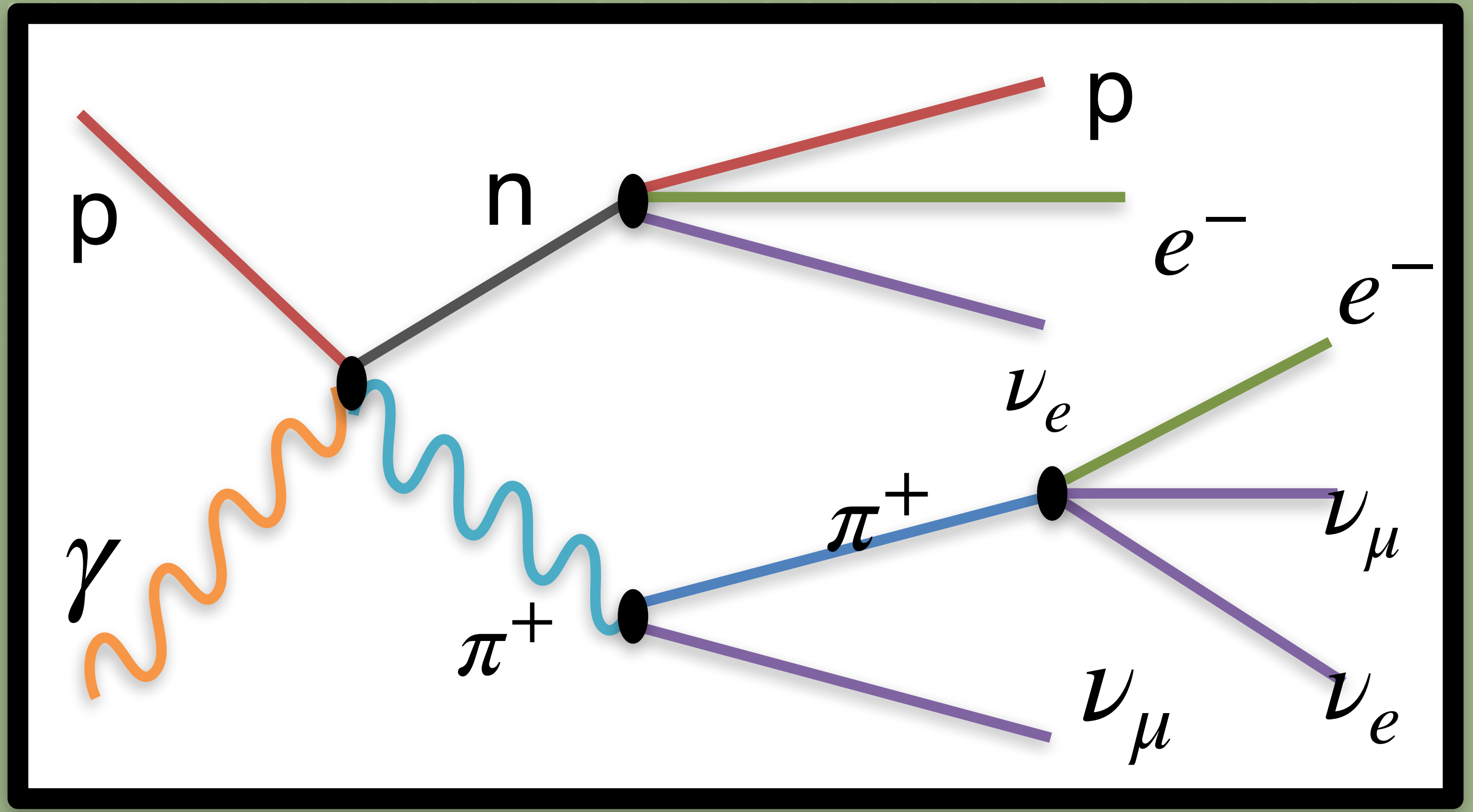

- Photo-pion production contributes to cooling for the proton population
- It also has the potential to produce observable neutrinos, but I will not be showing neutrino spectra today.

Illustration adapted from: Jonas Heinze

Fokker-Planck Electron Transport Equation

Escape Injection

$$\frac{\partial N_e}{\partial t} = \frac{\partial^2}{\partial \gamma^2}\left(D_0 \gamma^2 N_e\right) - \frac{\partial}{\partial \gamma}\left(\left\langle \frac{d\gamma}{dt} \right\rangle N_e\right) - \frac{N_e \gamma D_0}{\tau} + \left.\frac{\partial N_e}{\partial t}\right|_{\rm inj}$$

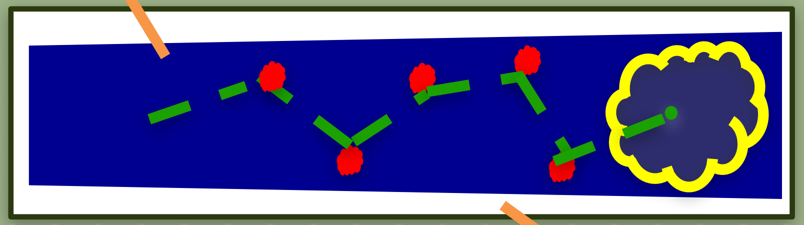

$$\left\langle \frac{d\gamma}{dt} \right\rangle = D_0\left(4\gamma + a\gamma - b_{\rm syn}\gamma^2 - b_{\rm C}\gamma^2\right)$$

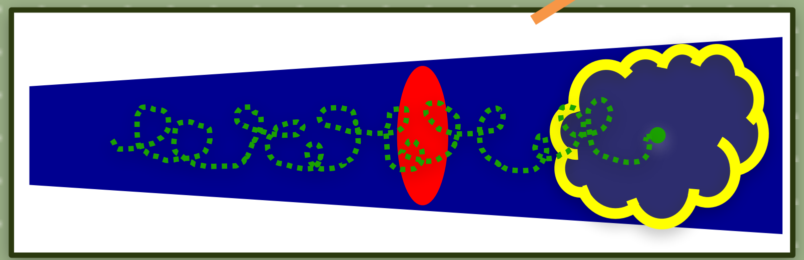

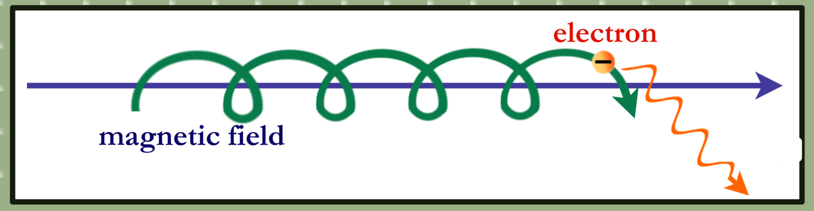

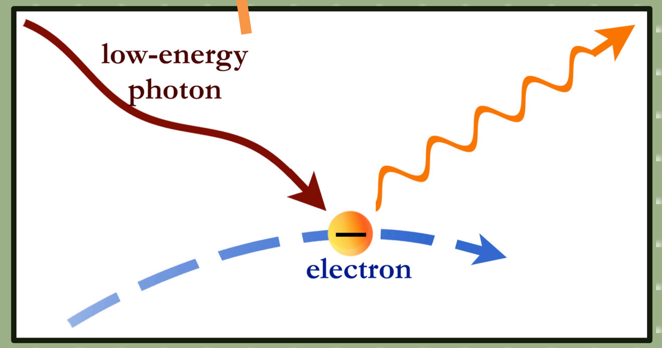

- N is the number of electrons with respect to the electron Lorentz factor.
- This version of the equation can be solved analytically, although generally I employ a more accurate accounting of the inverse Compton processes.
- An analogous equation is solved for the proton population.

Lewis, Becker & Finke (2016)

A Simplified Analytic Electron Distribution with Explicit Physics

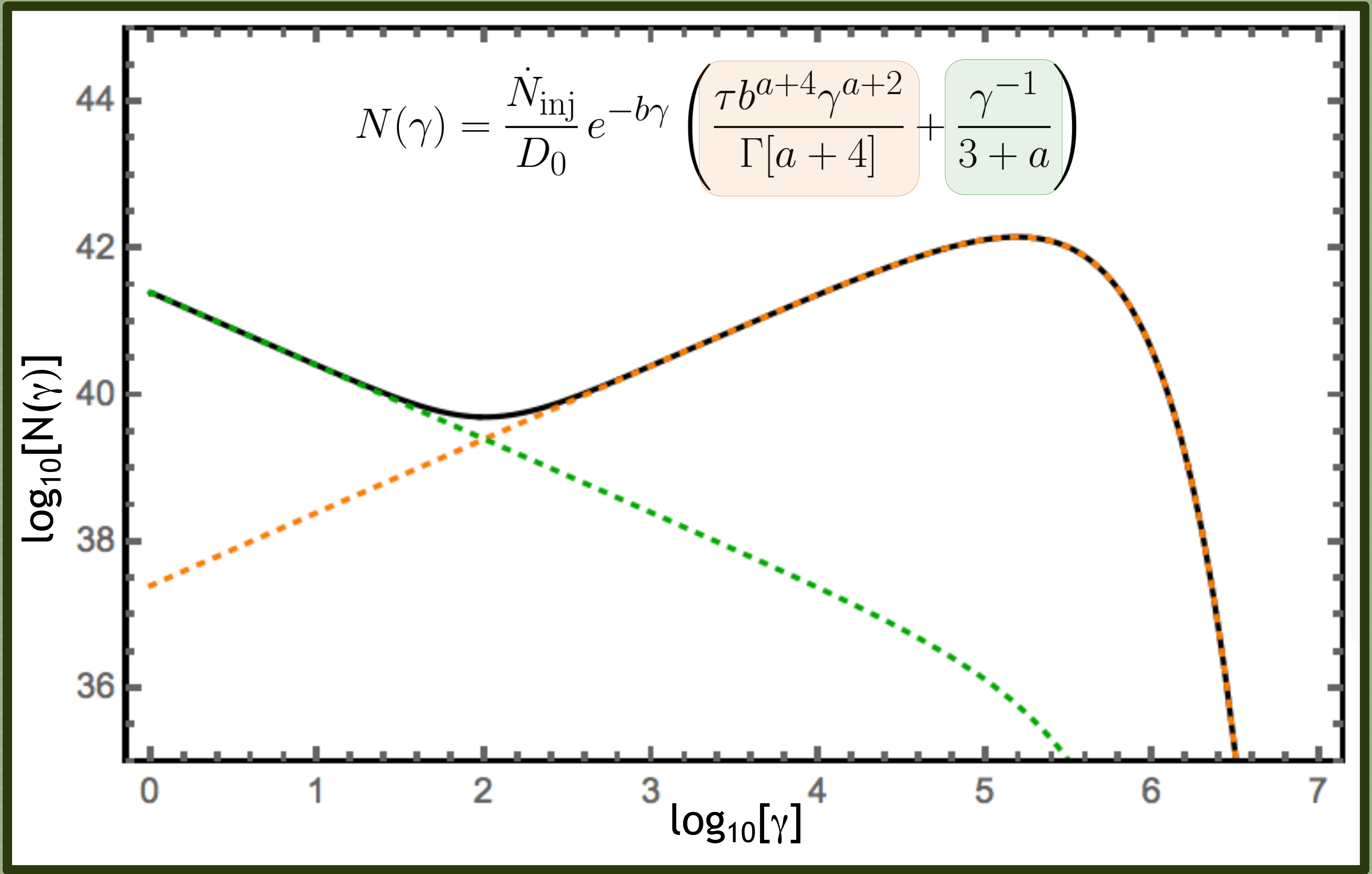

- Orange: balance between Fermi I and Fermi II terms
- Green: dominated by Fermi II acceleration
- These components of the analytic solution are NOT separable

Lewis et al. (2019)

How Acceleration Processes Impact Spectral Features

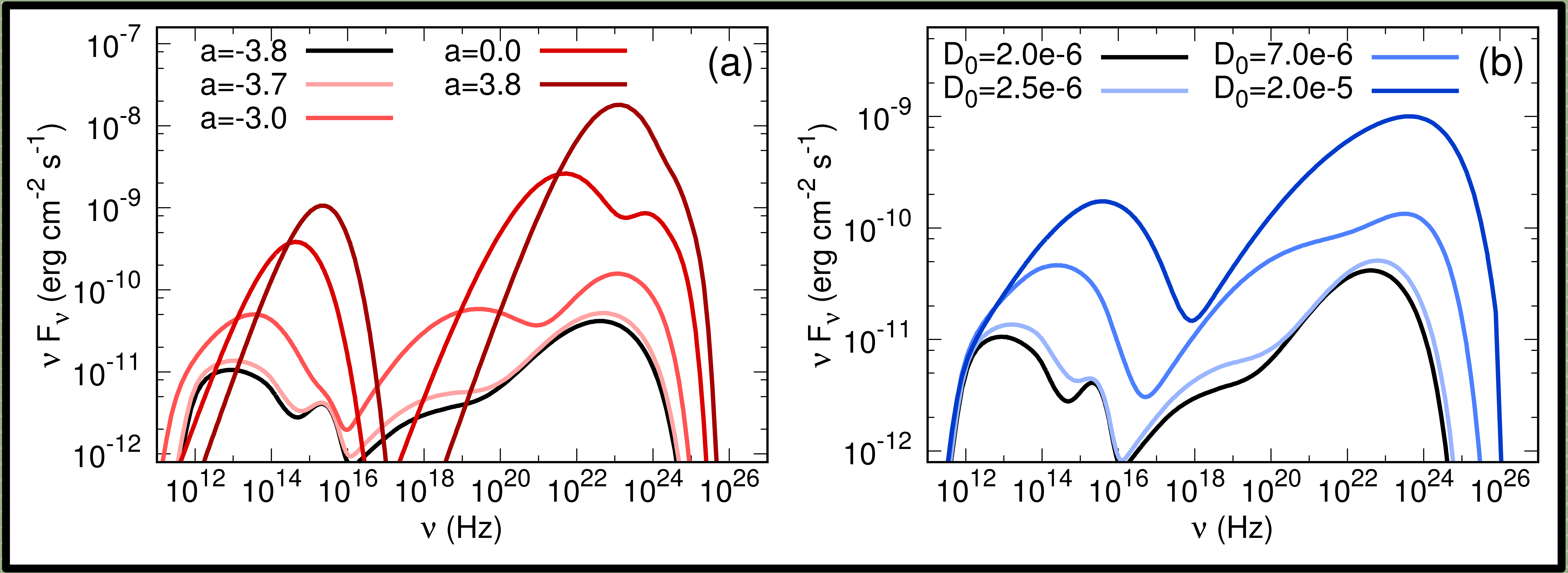

Fermi-I (shock) acceleration:
As red intensifies, the shock increases

Fermi-II (stochastic) acceleration
As blue intensifies, Fermi-II increases

The black spectrum is the same in both panels.

Lewis, Finke, & Becker (2018)

Particle Energy Distributions Impact Spectra

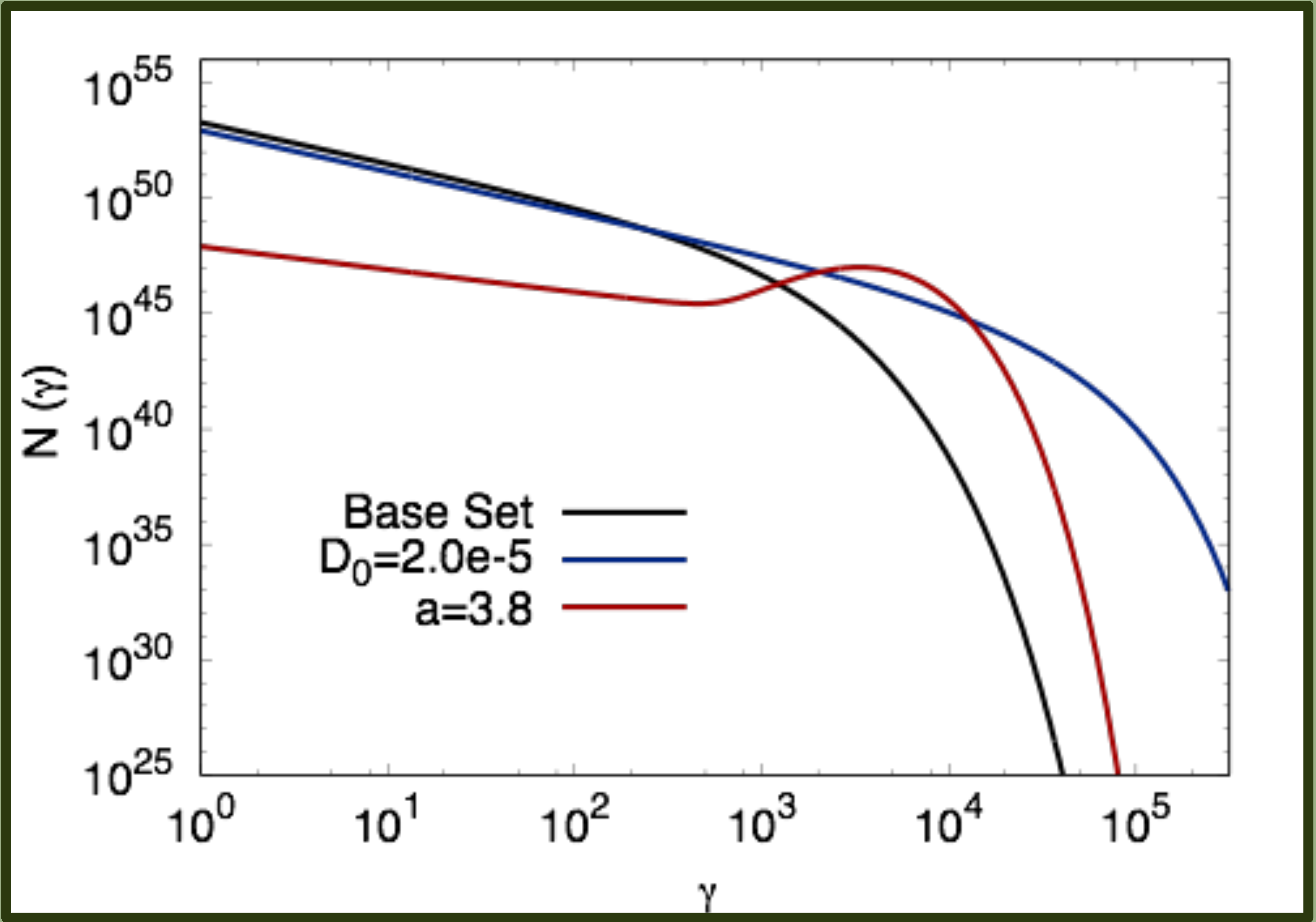

Lewis, Finke, & Becker (2018)

The spectral shape is dictated in part by the shape of the particle spectrum.

Particles accumulating at higher energies lead to sharper peaked spectra.

Historical TXS 0506+056 Data

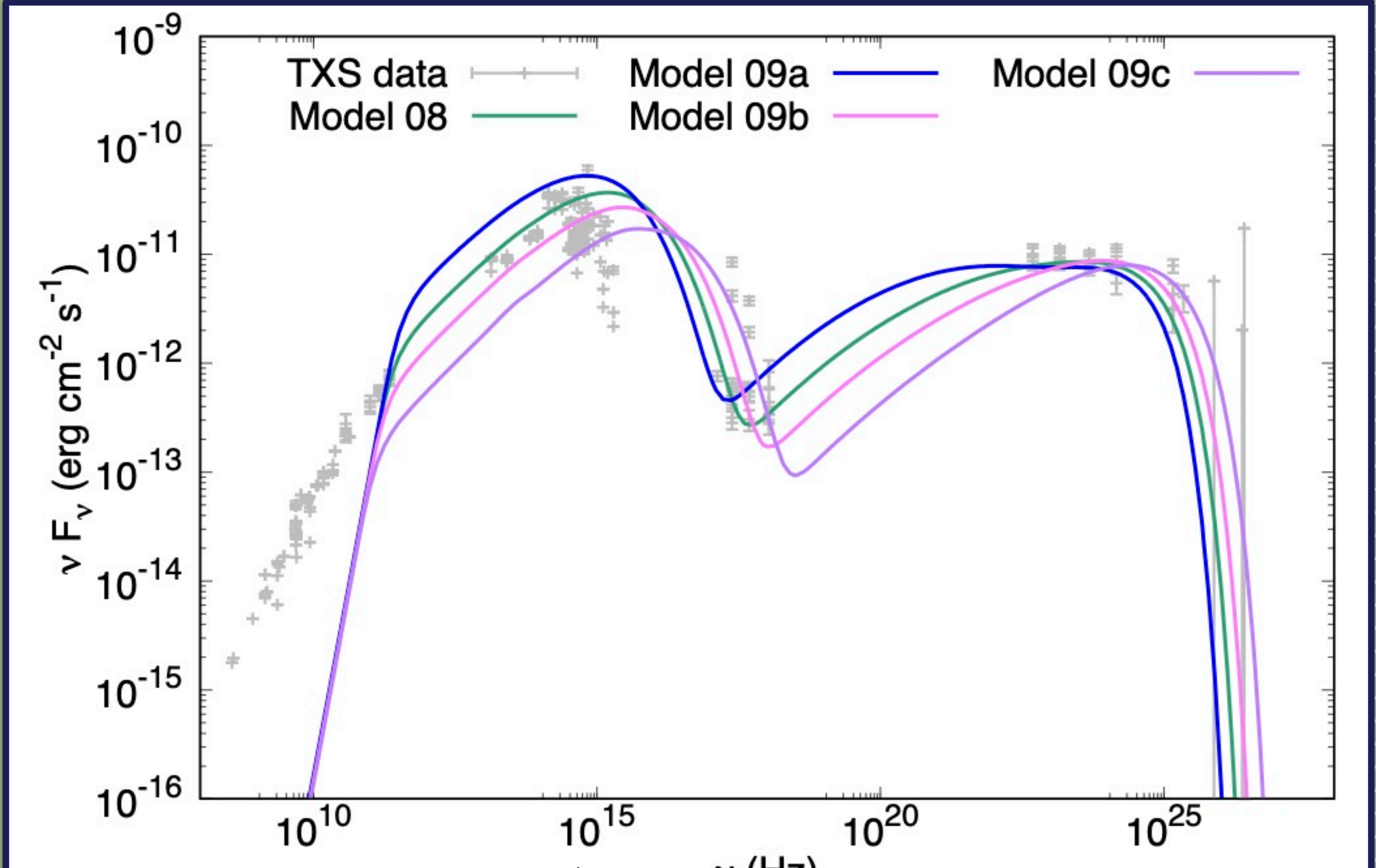

arXiv:2111.10600; submitting to ApJ)

- Comparison to historical data to constrain the base-line parameter space
- It is only necessary to change a single parameter to illustrate this range of data
- B is varied from 0.5 to 1.2 G

TXS 0506+056 Data: the 2014-2015 Neutrino Flare

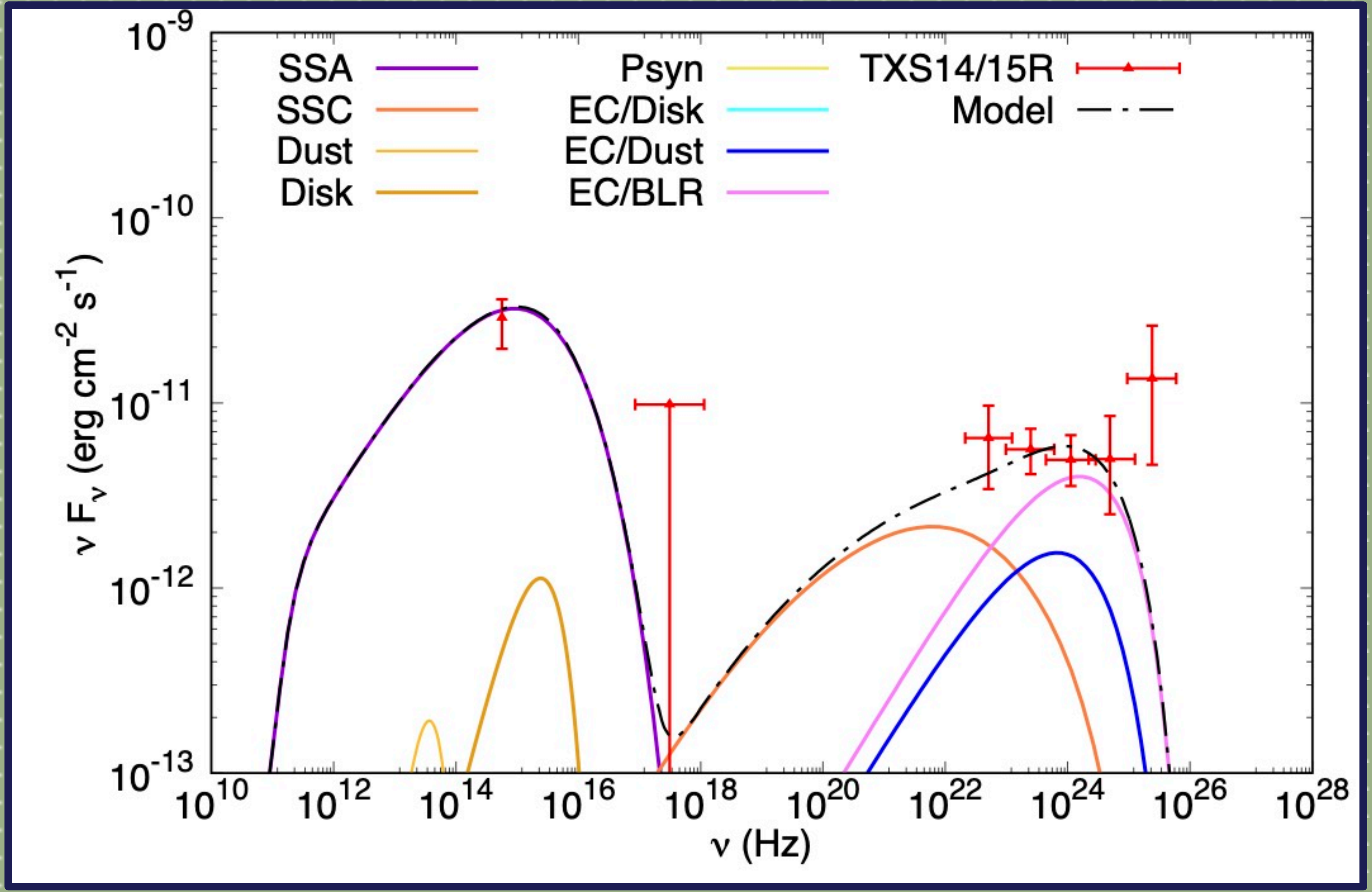

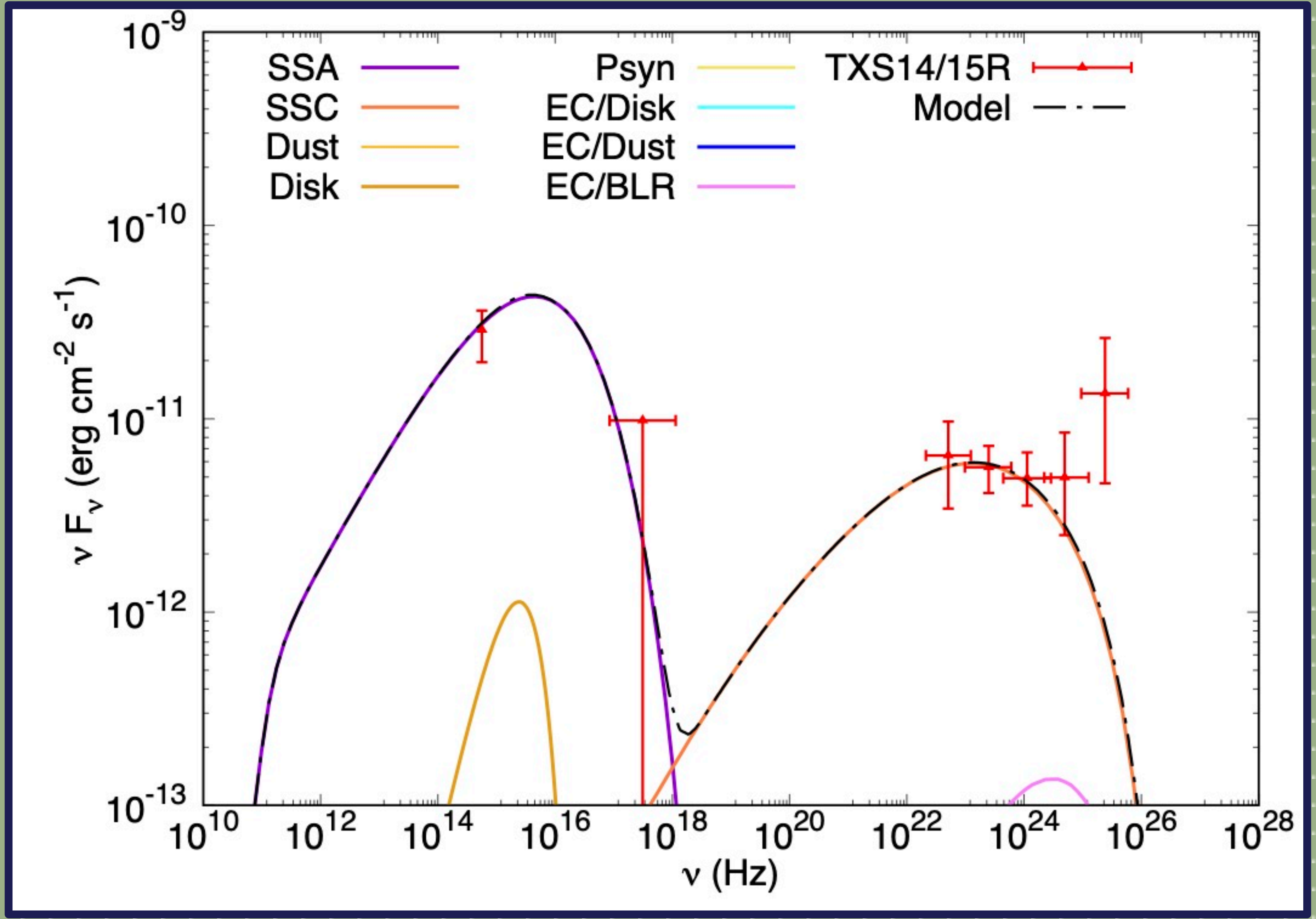

- Comparison of the FSRQ leptonic model to multiwavelngth flare data
- The model is tuned such that external Compton dominates in the γ-rays.

- Comparison of the BLL leptonic model to multiwavelngth data
- The model is tuned such that synchrotron self-Compton dominates in the γ-rays.

arXiv:2111.10600; submitting to ApJ; Data: Rodrigues et al. 2019

2014 Neutrino Flare MeV Spectra for AMEGO-X

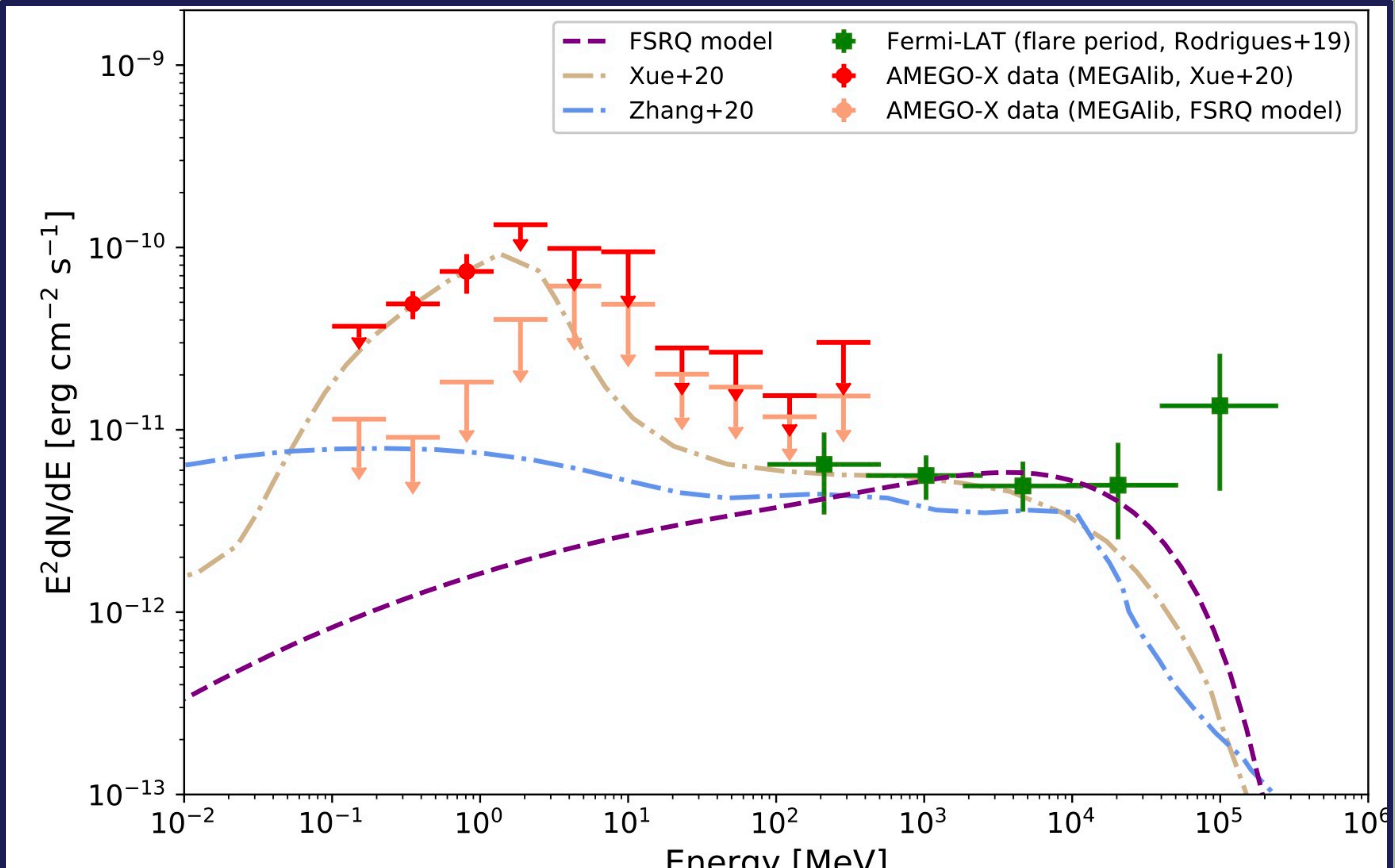

arXiv:2111.10600; submitting to ApJ)

(arxiv:2208.04990; accepted to JATIS)

In the figure:

- Fermi LAT data is in green
- Simulated AMEGO-X data in red & peach
- 3 leptohadronic models representing different dominant emission processes.
  - Purple is Inverse Compton
  - Blue is hadronic cascades
  - Tan is 2 zones with coronal gamma-gamma absorbed cascade emission in the MeV, but inverse Compton in the GeV

AMEGO-X would have detected the tan model or ruled it out through non-detection.

COSI Will Also Observe Blazars

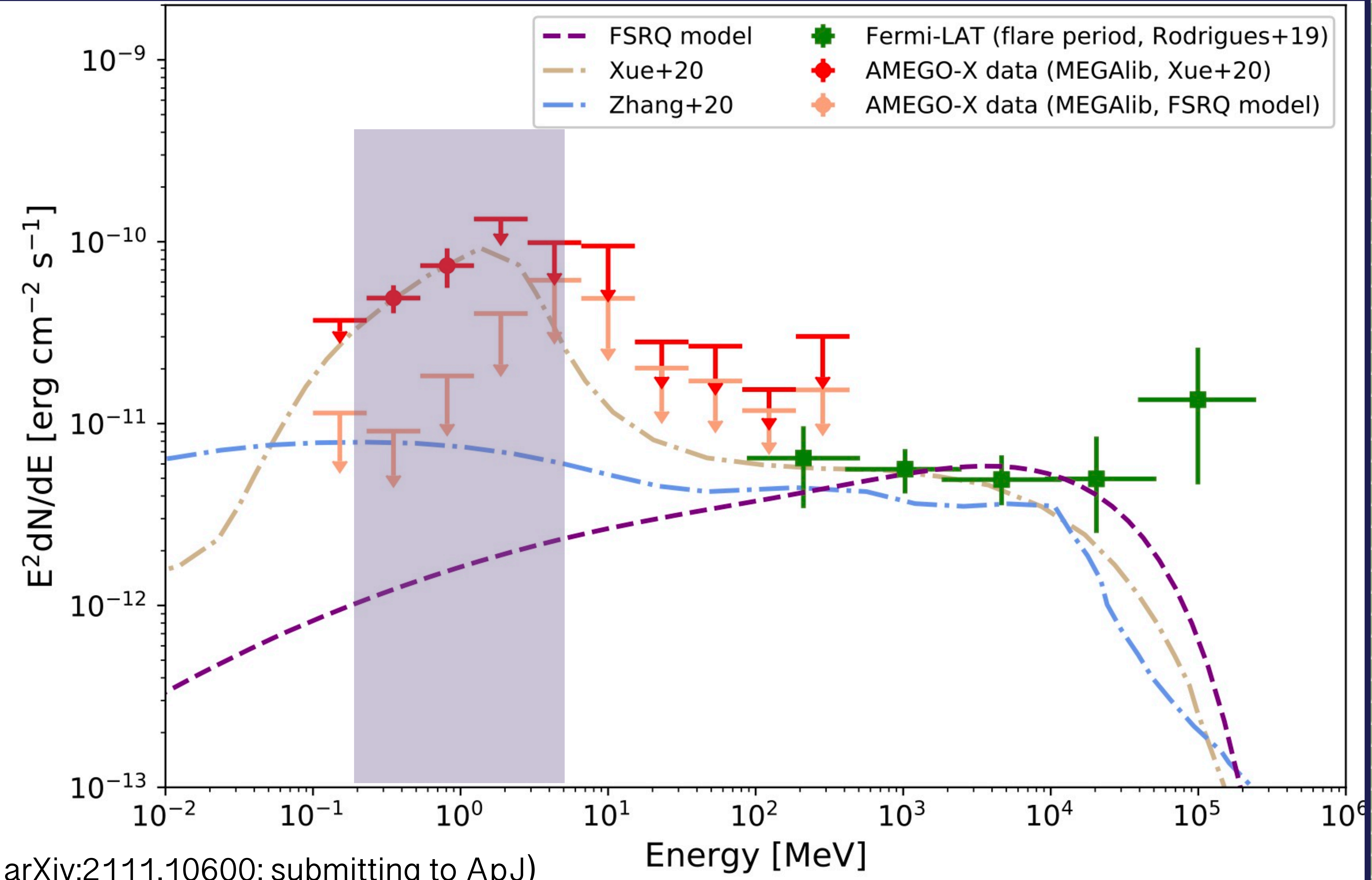

arXiv:2111.10600; submitting to ApJ)

The purple box, containing the peak of the tan model, is COSI's sensitivity band.

- COSI is a large field of view 0.2-5 MeV gamma-ray satellite mission planned for launch in 2026 (Tomsick et al., arXiv:1908.04334, arXiv:2109.10403)
- COSI is expected to detect flares from ~35 blazars/year & a correlation study with IceCube events is planned

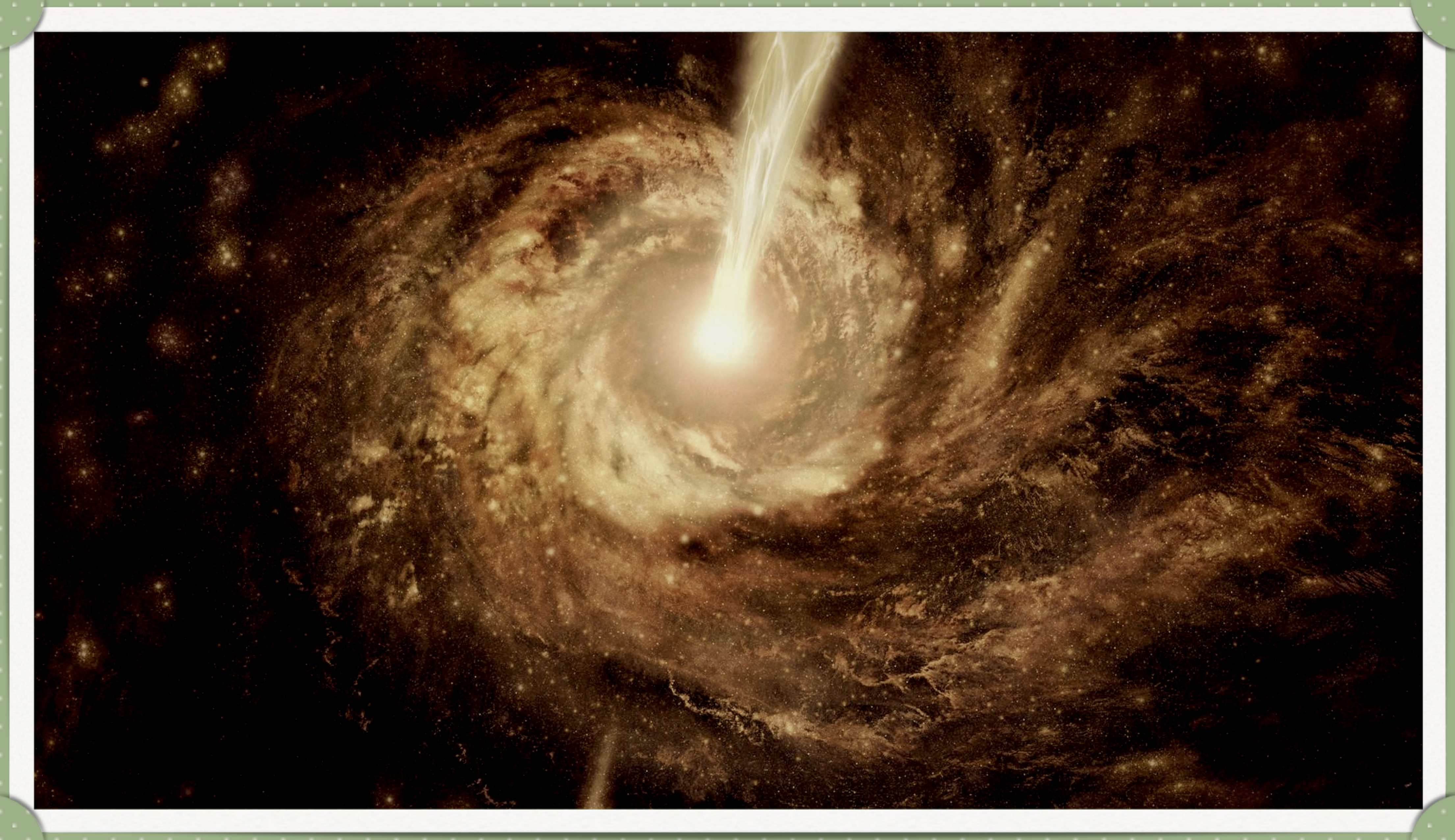

Questions?

Dr. Lewis's research was supported by an appointment to the NASA Postdoctoral Program at the NASA Goddard Space Flight, administered by Oak Ridge Associated Universities under contract with NASA.

H.F. acknowledges support by NASA under award number 80GSFC21M0002. Any opinions, findings, and conclusions or recommendations expressed in this material are those of the author(s) and do not necessarily reflect the views of the National Aeronautics and Space Administration.

References:

Lewis, T. et al. 2021, Modeling and Simulations of TXS 0506+056 Neutrino Events in the MeV Band, https://doi.org/10.48550/arXiv.2111.10600

Rodrigues, X., Gao, S., Fedynitch, A., Palladino, A.,& Winter, W. 2019a, ApJL, 874, L29, doi: 10.3847/2041-8213/ab1267
—. 2019b, ApJL, 874, L29, doi: 10.3847/2041-8213/ab1267

Xue, R., Liu, R.-Y., Wang, Z.-R., Ding, N., & Wang, X.-Y. 2021a, ApJ, 906, 51, doi: 10.3847/1538-4357/abc886

Zhang, B. T., Petropoulou, M., Murase, K., & Oikonomou, F. 2020, ApJ, 889, 118, doi: 10.3847/1538-4357/ab659a